Int J Clin Exp Pathol 2016;9(11):10853-10870
www.ijcep.com /ISSN:1936-2625/IJCEP0039643

Original Article

Anti-senescence role of coenzyme Q10 and 17 β-estradiol on submandibular gland of ovariectomized rats: histological, immunohistogical and molecular studies

Eetmad A Arafat[1,2], Fatma M Ghoneim[1], Hanaa A Khalaf[1], Ayman Z Elsamanoudy[3,4]

Departments of [1]Histology and Cell Biology, [4]Medical Biochemistry and Molecular Biology, Faculty of Medicine, Mansoura University, Egypt; [2]Department of Anatomy, Taif University, Saudi Arabia; [3]Clinical Biochemistry, Faculty of Medicine, King Abdulaziz University, Saudi Arabia

Received September 7, 2016; Accepted October 28, 2016; Epub November 1, 2016; Published November 15, 2016

Abstract: Decreased salivary secretion and diminished taste sensation are common symptoms in female at menopause or after surgical ovariectomy at any age. The aim of the study is to investigate the histological, immunohistochemical and molecular changes of the submandibular gland in a rat model of menopause and the possible protective effect of combined coenzyme Q10 and estrogen compared to estrogen therapy alone. Fifty adult female rats were used. They were classified into 5 equal groups: negative control (I), positive control receiving coenzyme Q10 (II), ovariectomized (III), ovariectomized and received estrogen (IV) as well as ovariectomized and received both estrogen and coenzyme Q10 (V). After 8 weeks the submandibular glands were dissected out for histological and α SMA immunohistochemical assessment. SMP-30 gene expression was also carried out. Moreover, measurement of lipid peroxidation product and total antioxidant capacity were done. The study revealed that ovariectomy induces oxidative stress of the submandibular gland in the form of increased oxidative stress markers, decreased SMP-30 mRNA gene expression, increased optical density of α SMA and ultrastructure degenerative changes. Slight improvement of these results is observed in estrogen treated group. In contrary, nearly complete recovery is noticed in combined estrogen and coenzyme Q10 treated group. We concluded that ovariectomy could induce submandibular gland cellular senescence and oxidative stress dependent histological changes. Estrogen has a protective role but combined coenzyme Q10 and estrogen therapy could have a better effect in prevention and protection against ovariectomy induced submandibular gland damage.

Keywords: Submandibular gland, ovariectomy, estrogen, cocoenzyme Q10, histological, molecular study

Introduction

Female menopause is the physiological process that happens at ages 45~55 years. It is defined as stoppage of menstruation for at least 6 months or more. It may occur also at any age after surgical ovariectomy. Beside the common symptoms of menopause, some oral manifestations usually develop, such as decreased salivary secretion and diminished taste sensation [1, 2].

It was documented that menopause is accompanied by a reduction in the salivary secretion from the submandibular and sublingual salivary glands as well as lowered estrogen levels [3]. This problem is improved by estrogen therapy (ET) [4]. So, xerostomia with or without a decrease in saliva volume is considered the major oral symptoms of menopause [5].

Cellular senescence is defined as a process limiting somatic cell proliferation that acts by disrupting cell division, loss of replication of nuclear DNA and increased expression of many tumor suppressor genes [6]. Moreover, it is characterized by alteration of cellular function [7, 8].

Senescence marker protein-30 (SMP30) is 30-KDa protein. Its expression levels decrease with the advanced age. It was reported that this protein is expressed in many organs of human,

mice and rats such as kidney, pancreas, skeletal muscle, and brain. In experimental study, gene transfer into cultured cells revealed that SMP30 is incorporated in the intracellular Ca2+ homeostasis. It acts by increasing calmodulin-dependent cell membrane-Ca2+-pump activity [9, 10]. Another studies established that SMP-30 has antioxidant effect [11, 12] and antiapoptotic effect [13]. SMP30 mediates a signal transduction pathway for selective membrane transport of electrolytes in the submandibular duct system [10].

It was postulated that cellular senescence could play a pathophysiologic role in menopause related symptoms as it was documented that SMP30 mRNA levels were significantly lower in ovariectomized rat in an experimental study [12].

Coenzyme Q10 (CoQ10) is a lipid soluble electron transporter. It transports electrons from complexes I and II to complex III in the mitochondrial electron transfer chain [14]. It is one of the major cellular antioxidants [15]. It was documented that there is a gradual, age-related decrease in the tissue levels and activity of CoQ10. Deficiency and/or mutations of genes involved in its synthesis are usually associated with disorders involving mitochondrial dysfunction in the nervous system, skeletal muscles, endocrine glands [16] and salivary glands [17]. Compromised status of coenzyme Q10 is a common finding in menopause [18].

The exact mechanism by which estrogen deficiency can induce dysfunction of the salivary gland is under debate. Moreover, whether hormonal replacement therapy (HRT) alone or its combination with other protective agents may be beneficial to the salivary gland is still uncertain. So, the current study aims to investigate the cell senescence and oxidative stress as a pathophysiologic mechanism mediating changes of the submandibular gland in a rat model of menopause and how is this reflected on the histology of the gland? Moreover, it aims to study the possible protective effect of coenzyme Q10 administration in combination with HRT compared to HRT alone.

Materials and methods

Chemicals

Estrogen was used as 17 β-estradiol (E2) produced by sigma Aldrich. It was dissolved in sesame oil and injected subcutaneously in a dose of (40 μg/kg/day) [19].

CoQ10 (C 9538, Sigma) was dissolved in sesame oil and injected subcutaneously in a dose of (22 mg/kg) [20].

Surgical ovariectomy

After one week of acclimatization the animals were anesthetized with 25 mg/kg thiopental sodium, injected intraperitoneally. A longitudinal incision (0.5-1 cm) was made in the midline area of the lower abdomen and the ovaries were removed. Aqueous penicillin (Cairo Company, Egypt) in a powder form was dissolved in distilled water and poured intraperitoneal before closing the incision. Then garamycin cream was applied locally as wound dressing for 7 days post-operative.

Sham operation

The abdominal cavities of control rats were opened but their ovaries were left intact, to be exposed to the same stress of the operation. The same antiseptic precautions and the same way of wound closure were followed as in ovariectomy group.

Experimental protocol

The protocol of this study was done in accordance with the Medical Research Ethics Committee of Mansoura University. A total of 50 adult female albino Sprague-Dawley rats (200-250 gm) were used in this study and they were kept in a quite environment for one week before study. The animals were housed in a room with optimal temperature and light-dark cycle. They were fed ad libitum and allowed free access to water during the experimental period. The rats were left for one week for acclimatization; then they were randomly divided into five equal groups (10 rats each): Group I (negative control group): rats were sham-operated and received the vehicle only for 8 weeks. Group II (positive control group): rats were sham-operated and received coenzyme Q10 (22 mg/kg/day S.C.) for 8 weeks. Group III (OVX): rats were bilaterally ovariectomized. Group IV (OVX+E2): rats were bilaterally ovariectomized and received E2 (40 μg/kg/day, s.c.) for 8 weeks. Group V (OVX+E2+ coenzyme Q10): rats were bilaterally ovariectomized and received both E2 and coenzyme Q10 for 8 weeks.

At the end of each experiment, all animals were sacrificed by ether anesthesia. The submandibular glands of one side were removed for histological and immunohistochemical study and the other side were used for molecular study.

Immunohistochemical (IHC) study

Paraffin-embedded sections were immunohistochemically stained using the avidin-biotin peroxidase system for the detection of actin fibers in the myoepithelial cells around the acini. The deparaffinized sections were rehydrated in ascending grades of ethanol then treated with 0.2% hydrogen peroxide in phosphate buffered saline for 30 min to block endogenous peroxidase activity. The sections were then incubated overnight in a humid chamber with the primary mouse monoclonal anti-αSMA antibody (clone 1A4; 1/50 dilution; Dako, Glostrup, Denmark). Sections were subsequently incubated with a second-stage biotinylated antibody (biotin-conjugated goat anti-rabbit IgG, 1:200, 1 h, at room temperature). 3, 3'-diaminobenzidine hydrogen peroxide was used as a chromogen. Finally, the sections were counterstained with haematoxylin dehydrated, and mounted. The immunoreactivity was visualized in the cytoplasm of myoepithelial cells. Positive and negative controls were included in each slide run and gave appropriate results [21, 22].

Electron microscopic study

The submandibular glands were obtained, cut into small fragments (about 1 mm^3), fixed in 2.5% buffered gluteraldehyde and then processed according to the standard procedures [23]. Toluidine blue stained semithin sections (1 μm thick) were used for fields' selection for examination by TEM. Uranyl acetate and lead citrate stained ultrathin sections were used for examination by JEOL 100 CX, Japan transmission electron microscope, Faculty of Science, Alexandria University, Egypt.

Assay of thiobarbituric acid reactive substances (TBARS) and total antioxidant capacity (TAC)

Submandibular glands of the other sides were dissected carefully from the 10 rats from each group. 40 mg of each gland was shock frozen for RNA extraction and the remaining part was carried to Petri dish. Then, they were transferred and washed with ice-cold isotonic saline. Homogenization of each gland was carried out in 0.1 mol/L Tris-HCl buffer, pH 7.4, at 4°C with a diluting factor of 4 using a Potter-Elvejhem homogenizer. Centrifugation of the homogenate was carried out at a 10000 *g* for 15 min in a cold centrifuge. Then, the supernatant was collected and stored at -20°C until measuring malondialdehyde levels and total antioxidant capacity (TAC).

Malondialdehyde level (the lipid peroxidation product) was estimated using thiobarbituric acid reactive substance (TBARS) method [24]. The results were measured as nanomoles per gram of tissue. TAC was assayed in tissue homogenizate [25]. The results were expressed as Trolox equivalents per gram wet tissue mass.

Quantitative real-time PCR (qRT-PCR) for determining the levels of gene expression

Immediately, after dissection of submandibular gland from each rat (10 rats per group), 40 mg gland's tissue was shock freeze with liquid nitrogen. Total RNA was extracted using Tri-Fast reagent (PeqLab. Biotechnologie GmbH, Carl-Thiersch St. 2B 91052 Erlongen, Germany, Cat. No. 30-2010), triazol, and chloroform.

The concentration and purity of the total RNA samples was examined by formaldehyde agarose gel electrophoresis as well as spectrophotometer measurement of its absorbance at 230, 260, and 280 nm (Genova Model; Jenway, UK). Ratios of (A260/A280 and A260/A230) equal or more than 1.8 indicate pure RNA samples.

Synthesis of cDNA from one mg of pure RNA was carried out using QIAGEN Long Range 2 Step RT-PCR Kit (100 reactions); (Germany, Cat. No. 205922): 20 μL reaction mix was prepared [2 μL of template extracted RNA, 9.8 μL DEPC treated water to Reverse-Transcription Master Mix that contains 4 μL Long Range RT Buffer (5×), 2 μL dNTP mix (10 mmol/L each), 1 μL Oligo-dT (20 μmol/L), 0.2 μL Long Range RNase inhibitor (4 U/μL), and 1 μL Long Range Reverse Transcriptase].

For synthesis of cDNA was carried out as follow; the master mix was vortexed for 5 s, incubated for 50 min at 42°C. Then, the enzyme was inactivated by heating at 85°C for 15 min. The synthesized cDNA was utilized for qRT-PCR of SMP30 against β-actin as an internal control

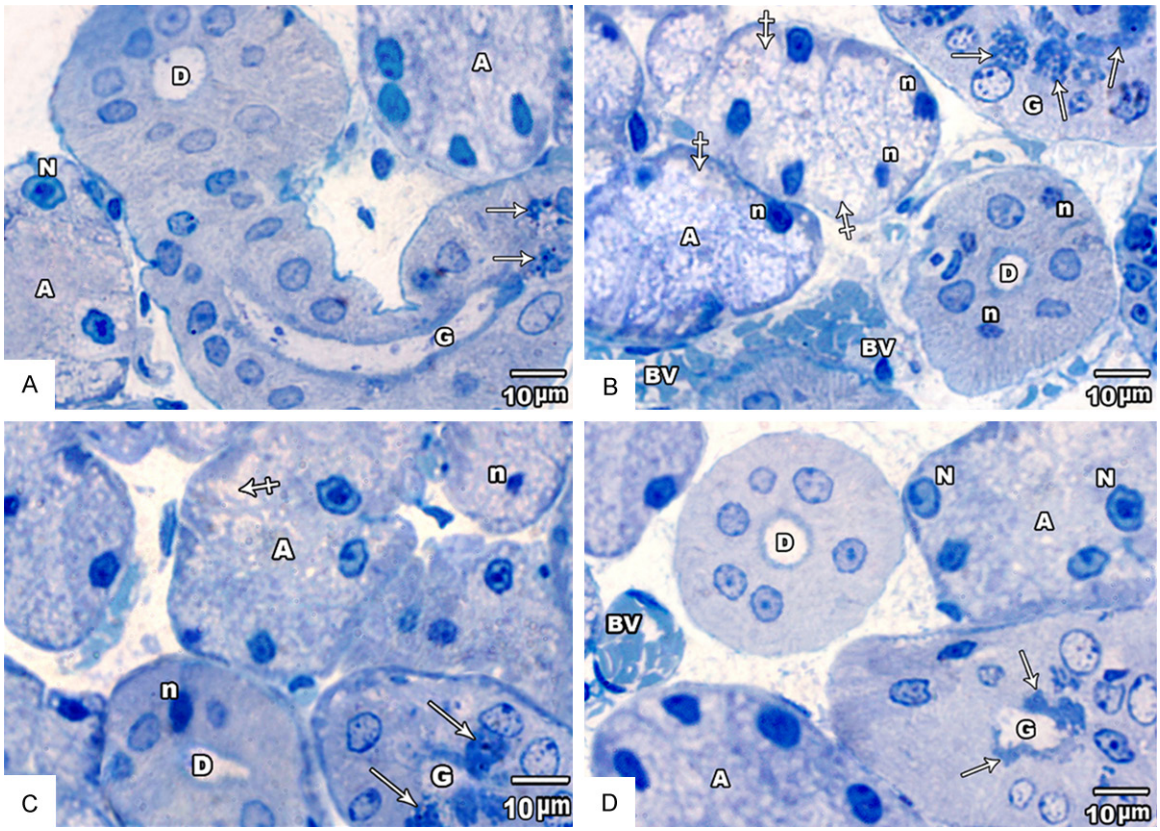

Figure 1. Photomicrographs of toluidine blue stained semithin sections of submandibular glands. A. (Control group) showing serous acini (A) with basal vesicular nuclei (N) and full of secretion. A granular convoluted tubule (G) with few apical granules (arrow) is seen connected to an intralobuolar duct (D). B. (Group III) showing pale serous acini (A) with small darkly stained nuclei (n) and cytoplasmic vacuolation (crossed arrow). The granular convoluted tubule (G) showing marked increased in the apical granules (arrow). An intralobular duct (D) with some pyknotic nuclei (n) and dilated congested blood vessel (BV) are also seen. C. (Group IV) showing acini with slightly vacuolated cytoplasm (crossed arrow). Both the acini (A) and the intralobular duct (D) showing few pyknotic nuclei (n). The granular convoluted tubule revealing increased amount of granules (arrow). D. (group V) showing normal histological picture of acini (A) with vesicular nuclei (N), GCT (G) with few apical granules (arrow) and duct (D). The connective tissue containing dilated congested blood vessel (BV). (Toluidine blue × 1000).

gene. The gene expression was performed using real-time polymerase chain reaction (qPCR) (7500 Fast Real-Time PCR System, Applied Biosystems, Foster City, CA, USA) and Sybr-Green reagent (SYBR Green PCR Master Mix-Applied Biosystems, USA, Cat. No. 4344463).

The sequences of the primers used: SMP30, forward: 5'-AGGCATCAAAGTGTCTGCTGTTT-3'; reverse: 5'-GACTGTCGAAGTGCCACTGAACT-3' (Huang et al. 2001). β-actin (97 bp; Gene accession numbers NM_031144.2), forward: 5'-ATGGTGGGTATGGGTCAG-3'; reverse: 5'-ATGCCGTGTTCAATGG-3' [26].

25 µL reaction mix for SMP30 was prepared; 1 µL of forward and reverse primers (10 pmol each), 12.5 µL Sybr-Green PCR Master Mix reaction buffer (Applied Biosystems), 2 µL cDNA and 8.5 DEPC treated water. qPCR was performed using a 7500 Fast Real-Time PCR System. 40 cycles at 95°C for 20 s, 60°C for 3 s and 60°C for 20 s were carried out according to the protocol previously described [27] for qRT-PCR of SMP30. The SMP30 expression gene was normalized to the expression of the housekeeping gene β-actin and the reactions were run in duplicate.

Melting curve analysis and 2% agarose gel electrophoresis were carried out to verify the specificity of the products generated for each primer pair. The quantification of the SMP 30 gene in each submandibular gland tissue sample was performed using a comparative method. β actin is used as endogenous housekeep-

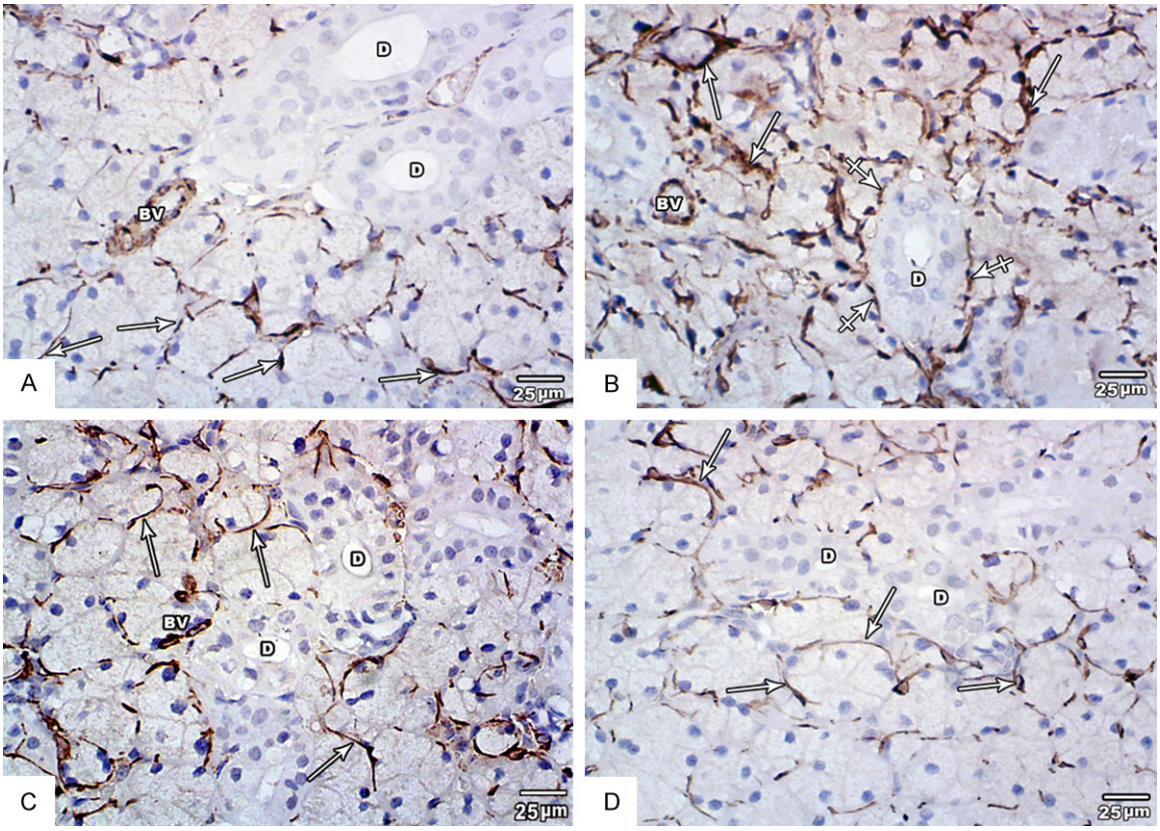

Figure 2. Photomicrographs of anti-alpha smooth muscle actin immunostained sections of submandibular glands. A. (Control group) showing moderate positive immune reaction in the myoepithelial cells (arrow) surrounding the acini (arrow) and in the wall of blood vessel (BV). Note absence of reaction around ducts (D). B. (Group II) showing a strong positive immune reaction around the acini (arrow) and blood vessel (BV). Notice the appearance positive immune reaction around the intralobular duct (crossed arrow). C. (Group III) showing slight decrease in the positive immune reaction around the acini (arrow) and in the wall of blood vessel (BV). Notice the absence of reaction around the duct (D). D. (Group IV) showing return of the reaction toward normal (Anti-alpha smooth muscle actin × 400).

ing control gene. Each analysis was done using 4 reactions (2 for analysis of the target SMP 30 gene and 2 for analysis of the internal housekeeping control gene, β actin). The ΔCT per each sample was calculated and linearized using $2^{-\Delta CT}$. Finally, ΔΔCT between studied groups in relation to the control samples were calculated and linearized using $2^{-\Delta\Delta CT}$ for overall change. Thus, the amount of target SMP 30 gene in the studied groups normalized to an endogenous reference (β actin) and relative to control group is given by anarithmetic formula. Estimation of ΔΔCT indicated the fold change in SMP 30 gene expression in the studied groups relative to the control group.

Morphometric study

Quantitative morphometric measurements of the optical density of α-SMA immunoreactivity were carried out blindly using ten non-overlapping fields from each animal at magnification × 400. The chosen fields were free from blood vessels.

The morphometric measurements were carried out on photographed slides using software system. Olympus digital camera (E24-10 mega pixel-China) installed on Olympus® microscope with 0.5× photo adaptor was used in photography. The result images were analyzed on Intel® Core® 13based computer using Video Test Morphology® software (Russian Federation, Saint-Petersburg, Russia).

Statistical analysis

All quantitative data were expressed as means ± standard deviation. In the statistical comparison between the different groups, the signifi-

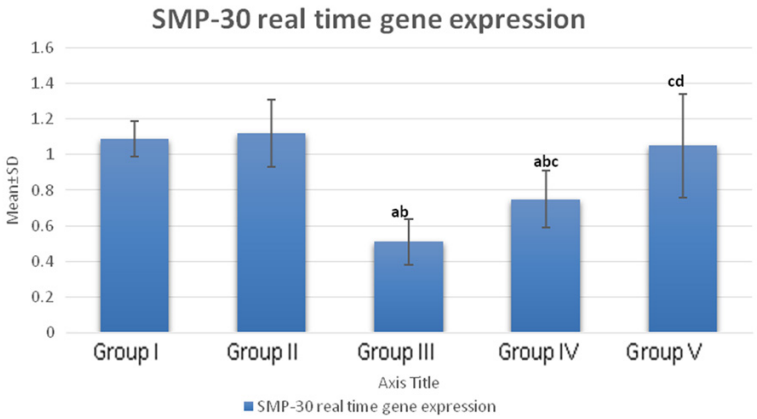

Histogram 1. mRNA real time RT-PCR gene expression of SMP-30 in the submandibular gland of the studied groups. Data expressed as mean ± SD. P: Probabilty. Test used: One way ANOVA followed by post-hoc tukey. a: Significant relative to group (I). b: Significant relative to group (II). c: Significant relative group (III). d: Significant relative to (IV).

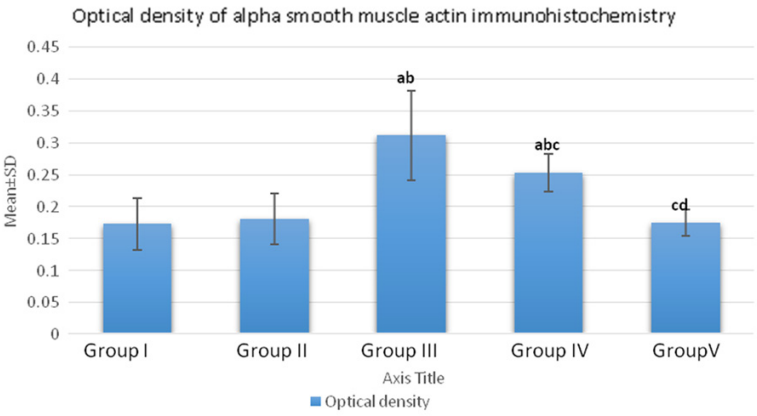

Histogram 2. Optical density of alpha smooth muscle actin immunohistochemistry in the submandibular gland of the studied groups. Data expressed as mean ± SD. P: Probabilty. Test used: One way ANOVA followed by post-hoc tukey. a: Significant relative to group (I). b: Significant relative to group (II). c: Significant relative group (III). d: significant relative to (IV).

cance of difference was tested using ANOVA (analysis of variance) to compare between more than two groups of numerical (parametric) data followed by post hoc Tukey for multiple comparisons using SPSS for Windows (15.0 Version). *P* value of less than 0.05 was considered statistically significant.

Results

Toluidine blue stained sections

Control groups (groups I & II): Examination of semithin sections stained with toluidine blue of all specimens in these groups was similar and revealed the normal histological structure specific for the submandibular gland including the secretory acini and the duct system. The secretory acini appeared with basal vesicular nuclei and full of secretion. The Granular convoluted tubules (GCT) were found close to the intralobuolar ducts. The granular cells lining the tubules were characterized by basal vesicular nuclei and apical deeply stained secretory granules (**Figure 1A**).

Ovarectomized group (group III): Examination of specimens from the ovarectomized animals revealed marked structural changes. The serous acinar cells appeared with small darkly stained nuclei and faintly stained cytoplasm containing variable sized vacuoles. An apparent increase in the apical granules of the granular convoluted tubules was observed. The acini were separated by connective tissue containing congested dilated blood vessels. Some pyknotic nuclei appeared in the intralobular duct (**Figure 1B**).

Ovarectomized group with estrogen replacement therapy (group IV): Examination of semithin sections of estrogen treated group showed that some acinar cells appeared with vesicular nuclei, while others had pyknotic nuclei and vacuolated cytoplasm but less than the ovariectomized group. The granular contents of the granular convoluted tubules were less than that of the ovariectomized group but more than the control one. Few pyknotic nuclei appeared in the intralobular duct (**Figure 1C**).

Ovarectomiezed group with both estrogen replacement therapy and Co enzyme Q (Group V): The SMG of the ovariectomized rats treated with estrogen and Co enzyme Q10 showed improvement of the degenerative changes reported in ovariectomized group. The acini, the

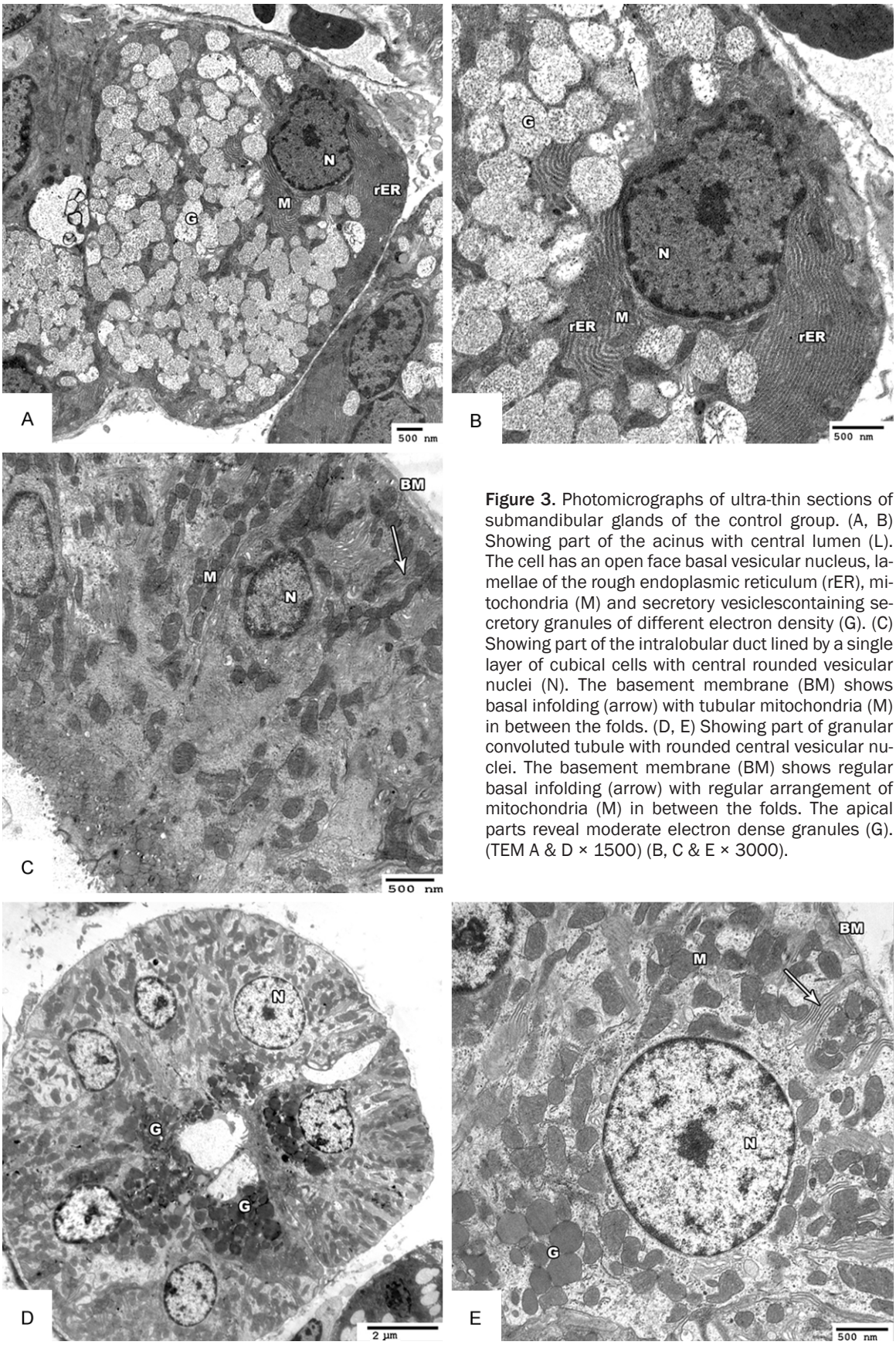

Figure 3. Photomicrographs of ultra-thin sections of submandibular glands of the control group. (A, B) Showing part of the acinus with central lumen (L). The cell has an open face basal vesicular nucleus, lamellae of the rough endoplasmic reticulum (rER), mitochondria (M) and secretory vesiclescontaining secretory granules of different electron density (G). (C) Showing part of the intralobular duct lined by a single layer of cubical cells with central rounded vesicular nuclei (N). The basement membrane (BM) shows basal infolding (arrow) with tubular mitochondria (M) in between the folds. (D, E) Showing part of granular convoluted tubule with rounded central vesicular nuclei. The basement membrane (BM) shows regular basal infolding (arrow) with regular arrangement of mitochondria (M) in between the folds. The apical parts reveal moderate electron dense granules (G). (TEM A & D × 1500) (B, C & E × 3000).

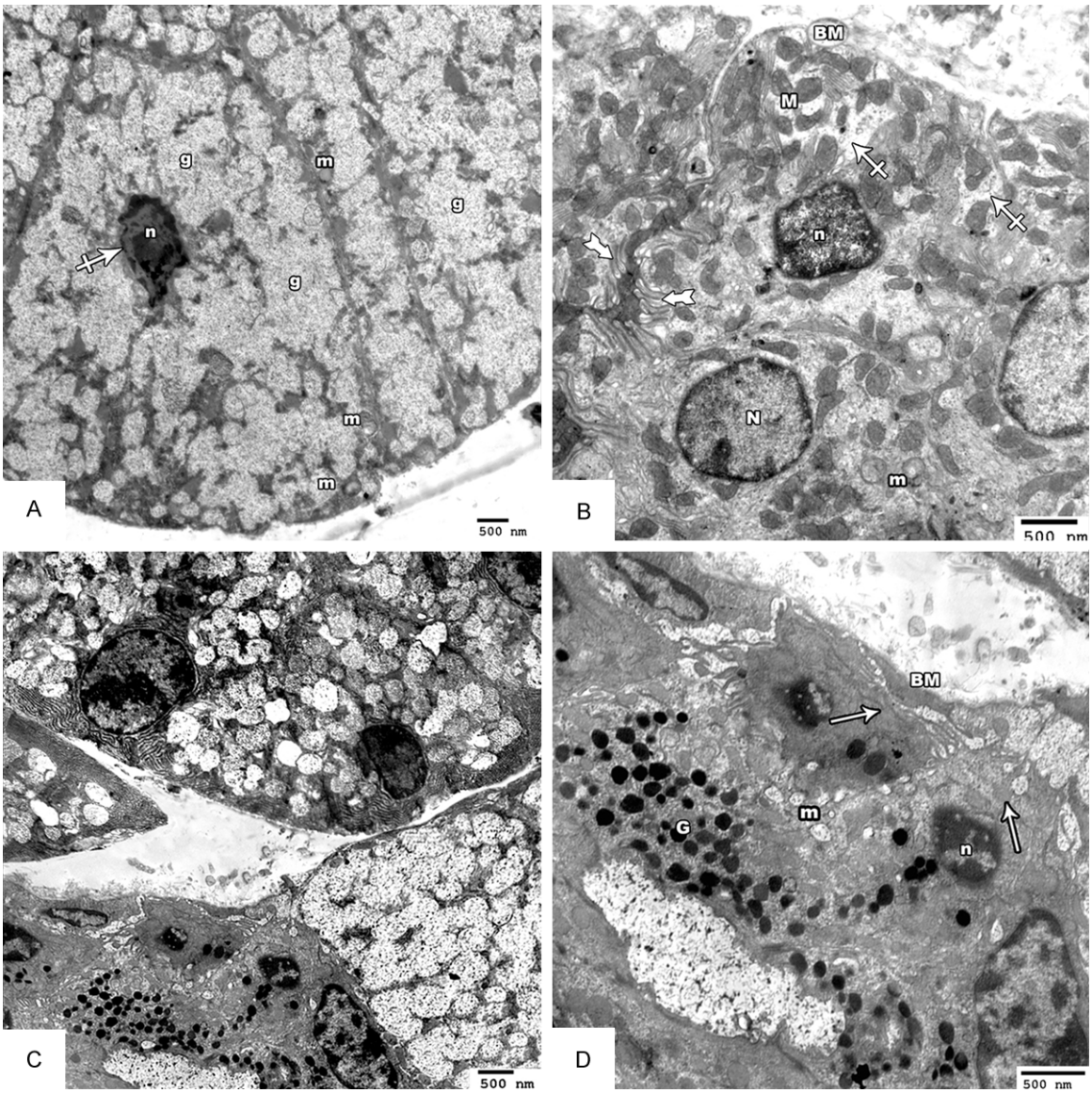

Figure 4. Photomicrographs of ultra-thin sections of submandibular glands of the OVX (group III). (A) Showing degeneration of acinar cells, shrunken hyperchromatic nucleus (n) with irregular nuclear membrane (arrow) and rupture of membrane organells, including the mitochondria (m) and the secretory granules (g) with degeneration of the rough endoplasmic reticulum. (B) Showing part of the intralobular duct lined by cells with vesicular nuclei (N) and other with small hyperchromatic irregular nucleus (n). The basement membrane (BM) shows area with lost basal infolding (crossed arrow) and other with irregular infolding (tailed arrow). The mitochondria are irregulary arranged and some showing mitochondrial vacuoles (m). (C, D) Shows part of GCT with small pyknotic nuclei (n), the basement membrane shows loss of basal infolding (arrow) and few small vacuolated mitochondria (m). The apical part reveals increased amount and density of the granules (G). (TEM A, B & D × 3000) (C × 1500).

duct system and the GCT were more or less similar to the control group (**Figure 1D**).

Immunohistochemically stained sections

A Positive immune reaction was seen in the myoepithelial cells surrounding the acini and in the wall of blood vessel of the control groups (**Figure 2A**). The OVX group (group III) showed significant increase in the optical density of the immune reaction around the acini and blood vessel with appearance of positive immune reaction around the intralobular duct (**Figure 2B**). Group IV showed significant decrease in the optical density of the immune reaction of myoepithelial cells around the acini compared with OVX group. In addition, absence of immune reaction around the duct was observed (**Figure**

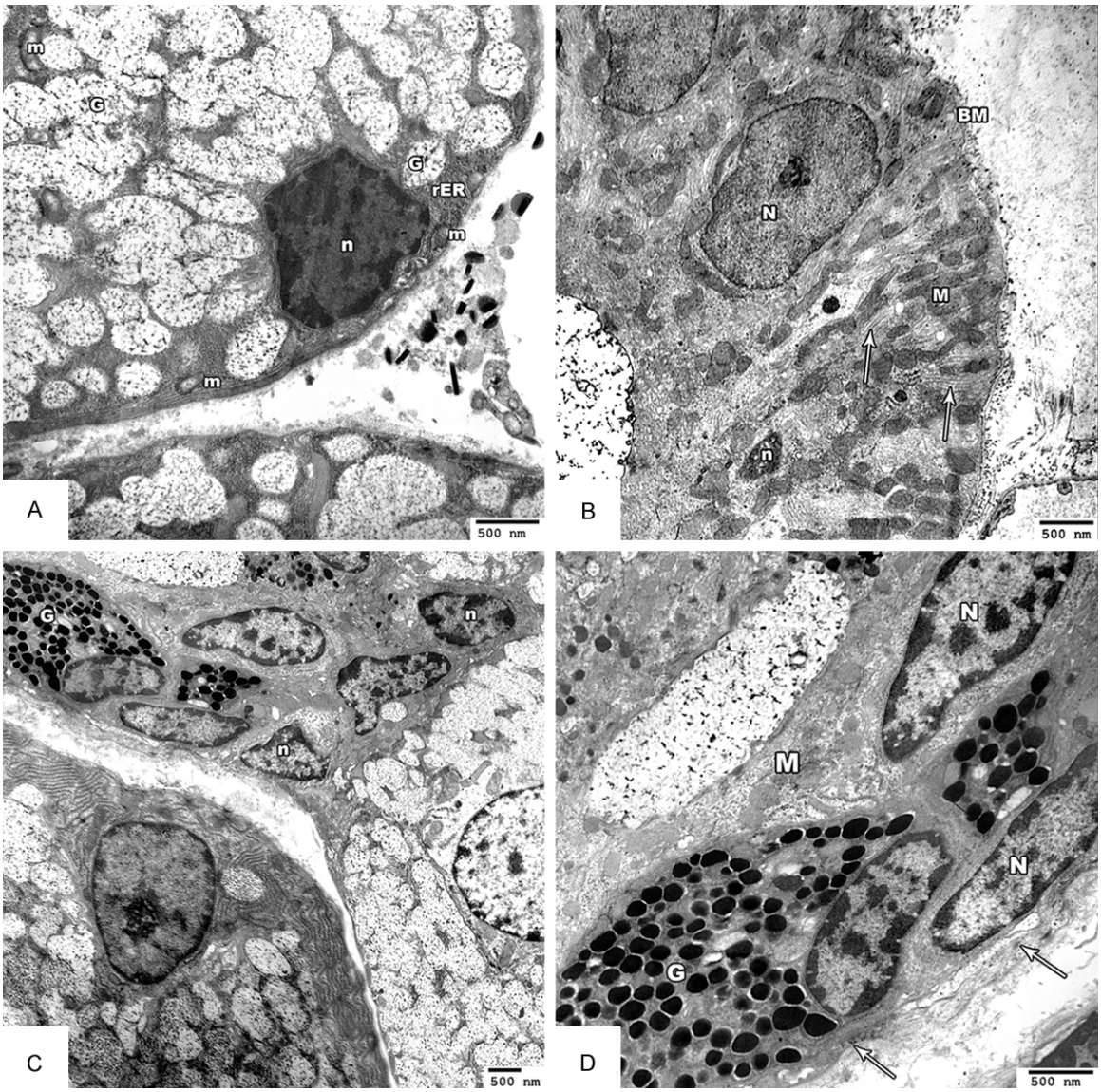

Figure 5. Photomicrographs of ultra-thin sections of submandibular glands of the estrogen treated OVX (group IV). (A) Showing the acini having normal sized hyperchromatic nucleus, appearance of few cisternae of rER, some vacuolated mitochondria and secretory vesicles containing few secretory granules. (B) A part of the intralobular duct showing a cell with vesicular nucleus (N) and other with small hyperchromatic nucleus (n). The basal membrane (BM) revealing regular basal infolding (arrow) and regular mitochondrial arrangement (M). (C, D) Showing part of GCT, the cells have vesicular nuclei (N), lost basal infolding (arrow) and irregular mitochondrial arrangement (M). The apical granules (G) revealing an increase in number and electron density. (TEM A, B & D × 3000) (C × 1500).

2C). Group V showed return of the optical density of the immune reaction of myoepithelial cells to normal (**Figure 2D**). A significant statistical decrease was observed between group V and IV (**Histogram 2**).

Electron microscopic results

Control groups (group I & II)

Electron microscopic examination of the submandibular glands of the control groups revealed the normal ultrastructure picture of SMG including the acinar cells with basal rounded vesicular nuclei, numerous cisternae of rER and mitochondria were seen in the basal part of the cells. Apical secretory vesicles containing secretory granules of different electron density were seen (**Figure 3A**, **3B**).

The striated duct cells were seen to have rounded vesicular nuclei. The basement membrane revealed basal infolding with numerous

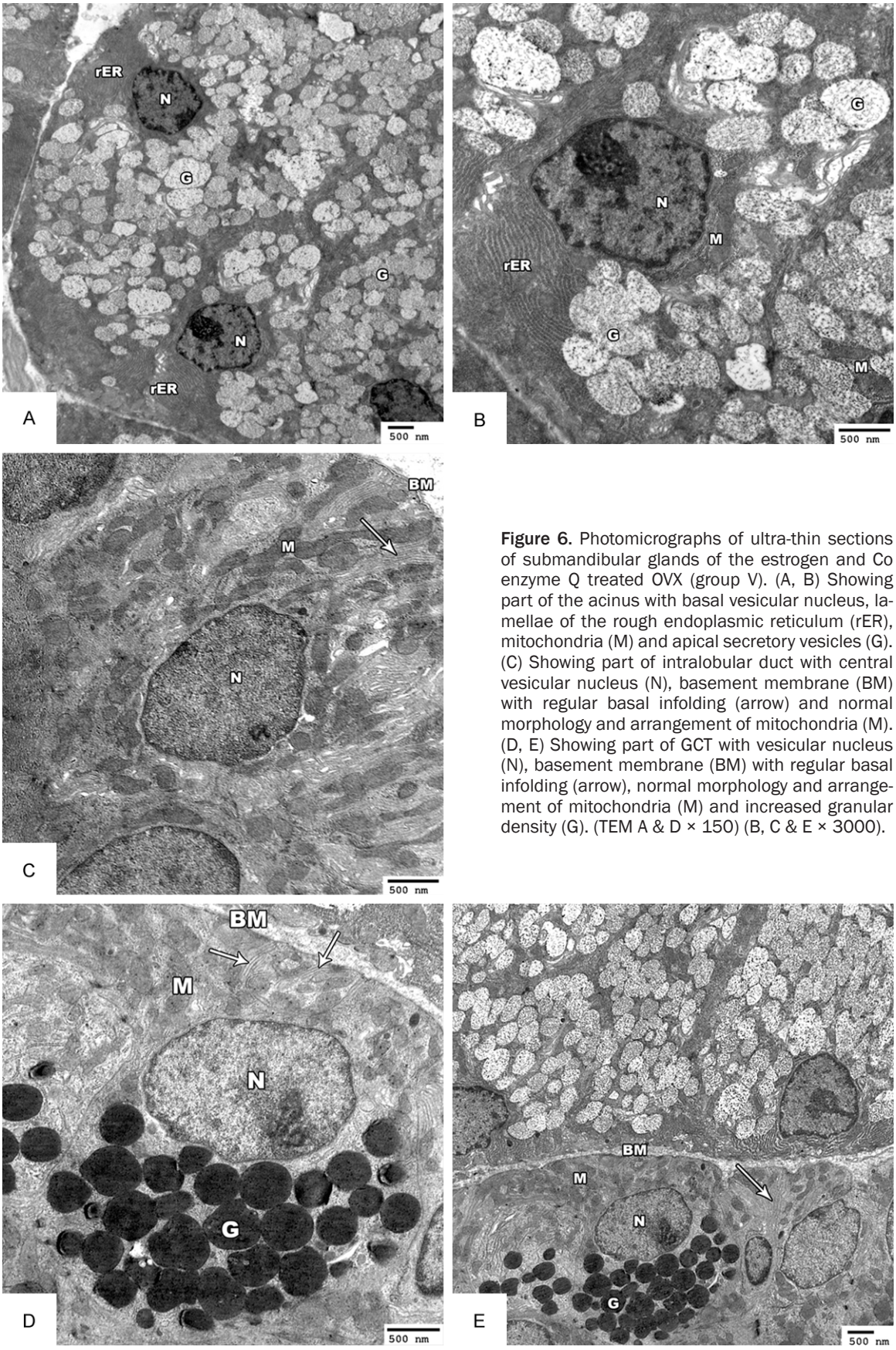

Figure 6. Photomicrographs of ultra-thin sections of submandibular glands of the estrogen and Co enzyme Q treated OVX (group V). (A, B) Showing part of the acinus with basal vesicular nucleus, lamellae of the rough endoplasmic reticulum (rER), mitochondria (M) and apical secretory vesicles (G). (C) Showing part of intralobular duct with central vesicular nucleus (N), basement membrane (BM) with regular basal infolding (arrow) and normal morphology and arrangement of mitochondria (M). (D, E) Showing part of GCT with vesicular nucleus (N), basement membrane (BM) with regular basal infolding (arrow), normal morphology and arrangement of mitochondria (M) and increased granular density (G). (TEM A & D × 150) (B, C & E × 3000).

Table 1. Oxidative stress markers of the submandibular gland in the studied groups

	Group I	Group II	Group III	Group IV	Group V	P
TBARS (nmol/mg)	2.45±0.42	2.31±0.37	5.6±1.01[a,b]	3.93±0.85[a,b,c]	2.97±0.73[c,d]	<0.001
TAC (Trolox equivalents per gram wet tissue weight)	3.79±0.87	3.84±0.99	1.61±0.48[a,b]	2.71±0.53[a,b,c]	3.76±0.84[c,d]	<0.001

Data expressed as mean ± SD. P: Probabilty. Test used: One way ANOVA followed by post-hoc tukey. a: significant relative to group (I). b: significant relative to group (II). c: significant relative group (III). d: significant relative to (IV).

elongated mitochondria in between. The apical parts revealed apical microvilli (**Figure 3C**).

The granular convoluted tubular cells of the submandibular glands of the control groups revealed regular basal infolding with basal mitochondria and the apical parts showed moderate electron dense granules. The nuclei were rounded and vesicular (**Figure 3D**, **3E**).

Ovarectomiezed group (group III)

Ultrastructure examination of the acinar cells of this group revealed marked degenerative changes in the form of hyperchromatic nuclei and irregular nuclear membrane. The cytoplasm showed destruction of membrane organelles, including the mitochondria, the secretory granules and the rough endoplasmic reticulum (**Figure 4A**).

The striated duct revealed some cells with vesicular nuclei and others with small hyperchromatic ones. The basal membrane showed areas with regular basal infolding, others with irregular infolding and third ones with lost basal infolding. The mitochondria were irregularly arranged and some showed mitochondrial vacuoles (**Figure 4B**).

The granular convoluted tubular cells revealed some cells with small hyperchromatic nuclei and irregular nuclear membrane. The basilar membrane showed areas of complete loss of basal infolding. Few small vacuolated mitochondria were also seen. The apical parts of the cells revealed numerous electron dense secretory granules (**Figure 4C**, **4D**).

Ovarectomiezed group with estrogen replacement therapy (group IV)

Electron microscopic examination of the submandibular glands of this group revealed partial recovery of the acinar cells. The cells had basal vesicular nuclei with irregular nuclear membrane, few cisternae of rER and mitochondria. The secretory granules were more electron lucent than those of the control (**Figure 5A**).

The striated duct revealed normal ultrastructural appearance apart from few pyknotic nuclei (**Figure 5B**).

The Granular convoluted tubules showed an apparent increase in their granular contents compared to the control group (**Figure 5C**, **5D**).

Ovarectomiezed group with both estrogen replacement therapy and Co enzyme Q (Group V)

The SMG of the ovariectomized group treated with estrogen and Co enzyme Q10 showed improvement of the degenerative changes reported in the ovariectomized group. The acini (**Figure 6A**, **6B**), duct system (**Figure 6C**) and the GCT (**Figure 6D**, **6E**) were more or less similar to the control group.

Statistical and morphometric results

Table 1 represents the oxidative stress markers of the submandibular glands in the studied groups. It shows increase in the markers of submandibular oxidative stress in the ovariectomized animals group (model group-III) in the form of increased lipid peroxiation product (TBRS) level with decreased total antioxidant capacity. These markers show reversed results in the treated groups (IV & V) which indicates lowered submandibular oxidative stress in the treated groups in comparison to the model group (III). Moreover, the group of combined treatment by E2 and Co Q10 (group V) presented decreased level of TBRS and increased total antioxidant capacity when it is compared to the E2 treated group (group IV).

Regarding SMP-30 mRNA real time gene expression, it is presented in **Histogram 1**. In ovariectomized animal group (III), there is a significant decrease in submandibular SMP-30 gene expression than the control groups (I & II). While, there is statistically significant increase in the treated groups (IV & V) than the model

group (III). Interestingly, there is statistically significant increase in the group of combined treatment by E2 and Co Q10 (group V) than E2 treated group (IV).

Regarding α SMA immunostaining, it is presented in **Histogram 2**. In the ovariectomized animal group (III), there is a significant increase in optical density of α SMA compared to the control groups (I & II). While, there is a statistically significant decrease in the treated groups (IV & V) than the model group (III). Interestingly, there is statistically significant decrease in the group of combined treatment by E2 and Co Q10 (group V) than E2 treated group (IV).

Discussion

As current treatment strategies of menopausal symptoms especially those resulted from cellular senescence are mainly limited to symptomatic and supportive care, more effective therapeutic options should be developed for better management of these disorders. Therefore, in this study, we aimed to discuss the effect of experimental ovariectomy on the submandibular gland and also to evaluate the effects of estrogen alone and together with Co enzyme10, a radical-scavenging antioxidant present in most eukaryotic cells, on the submandibular gland of OVX rat models at the molecular and histological aspects.

Our data signified that ovariectomy induced oxidative stress (increased MDA and lowered TAC). Moreover, SMP-30 gene expression (the senescence marker) showed marked decrease in those animals when compared to the control groups.

OVX is associated with oxidative stress with impaired redox balance [28]. Oxidative stress in OVX could be explained by sequestration of hydrogen polyunsaturated fatty acids [29] with activation of lipid peroxidation in cellular and subcellular membranes [30]. Peroxides of the polyunsaturated fatty acids generate MDA, the indicator of lipid peroxidation [31]. Moreover, oxidative stress that is associated with OVX may be caused also, by reduction of energy consumption [32], development of insulin resistance state as evidenced by decreased adiponectin level [33], increased triacylglycerol level [34] with decreased LDL receptors expression and activity [28]. Subclinical inflammation and consequently tissue injury associated with increased cytokines release is an associated condition of OVX [35].

The decreased expression of SMP-30 gene observed in the current study was reported previously in 2011 by Fukui et al. [12]. They reported a similar finding in their study of the effect of OVX on liver injury [12]. The association between ovariectomy and cellular senescence is also documented [36]. Cellular senescence in OVX is explained by loss of ovarian estrogen that may induce senescence through induction of generalized low grade chronic inflammation [36] and oxidative stress [37, 38].

The link between oxidative stress and cell senescence which is marked by down-regulation of SMP-30 expression was documented. Oxidative stress that occurred in OVX can stimulate Ca^{++} influx into the mitochondria and the nuclei of cells from the extracellular environment through cytoplasm or from the intracellular environment through the endoplasmic and sarcoplasmic reticulum membranes and channels [39, 40]. The dysregulation of the intracellular Ca^{++} homeostasis is also, a result of down regulation of SMP-30 gene expression and loss of its role in protecting the cell from cellular senescence and apoptosis [12, 41].

As a consequence of down regulation of SMP-30 gene expression, there is impairment of Ca^{++} signaling pathway leading to a decline in the salivary gland secretory activity and functions at the cellular level [42, 43]. This was reflected histologically in our study in the form of small darkly stained nuclei with faintly stained cytoplasm containing variable sized vacuoles in the acinar cell which are morphological biomarkers of cellular senescence as reported by [8, 43]. Moreover, previous authors reported that the percentage number of submandibular gland acini and ducts was decreased in ovariectomized rats [1]. They explained this by reduced activity of transcription of cell cycle mediators in ovariectomy with reduction of estrogen receptors expression.

The apical granules of GCT were apparently increased in ovariectomized animals in addition to dilated congested blood vessels and pyknotic nuclei in the interlobular ducts. Nearly similar findings were reported in the submandibular gland of ovariectomized rats [2, 44].

These findings were explained by decreased estrogen level after OVX and loss of its protective effect on salivary glands as they reported that OVX can induce cell atrophic changes, subcellular organelle lesions and upregulation of apoptotic gene expression at the level of acinar and ductal epithelium of the submandibular glands [2, 45]. Ovariectomy induced hypovacularization with consequent hypoxia and hypocellullarity of the glands resulting from estrogen deficiency may be a possible explanation [46-48].

For more study of the mechanism by which OVX could affect the submandibular glands, the expression of alpha smooth muscle actin (α SMA) protein was carried out in the current study by α SMA immunohistochemistry. The present study revealed increased α SMA immunoreactivity at the periphery of the acini and blood vessels. This reaction was localized in the myoepithelial cells surrounding the intralobular ducts.

The importance of α SMA as a myoepithelial cell marker in salivary gland physiology was well documented. It is a marker of myofibroblasts, immature progenitor and/or stem cells [49] and its expression is increased in response to stress and degeneration [50]. Disorder in its expression is associated with cytoskeletal disorganization and damage which is caused mainly by oxidative stress [51]. Alpha SMA expression and polymerization are increased in response to oxidative stress and there is a positive correlation between its expression at the cellular and circulatory levels and the oxidative stress markers; 8-oxo-7, 8-dihydro-2'-deoxyguanosine [52, 53]. Moreover, α SMA expression is more in senescent cell [54, 55], this result is confirmed in the current study.

So, ovariectomy through stimulating submandibular salivary gland oxidative stress could induce submandibular senescence which in turn recruit and retain myofibroblast and progenitor stem cell which is evidenced by increased expression of α SMA as a defense mechanism against marked cellular damage.

Ultrastructure examination of the submandibular gland of OVX group (II) showed multiple degenerative changes; the acini revealed irregular and hyperchromatic nuclei in addition to destruction of membranous organelles, including the mitochondria, the secretory granules and the rough endoplasmic reticulum. A similar ultrastructure changes were previously reported in both submandibular and lacrimal glands of OVX rats [2] and in the parotid acini of OVX rats [48]. They referred this degenerative changes to the oxidative stress resulted from estrogen deficiency. Estrogen which is one of the sex hormones is well known as a natural antioxidant. As it was reported that its serum level is directly proportional to the level of antioxidase and anti-oxidative activity, yet it has an inverse correlation with oxidative stress production [56, 57]. These findings indicate that estrogen deficiency may be responsible for the reduction in antioxidants and an increase in ROS. Therefore a close relationship may be present between the structural and functional menopausal changes and the oxidative stress caused by estrogen withdrawal.

In the current work, ultrastructural examination of the acini, ducts and glandular convoluted tubules showed vacuolation and irregular arrangement of mitochondria. These results come in accordance with [2].

The role of E2 as a replacement therapy after ovariectomy is well studied. E2 alone or in combination with other antioxidant supplements like vitamin E has a beneficial protective effect against OVX induced oxidative stress. It decreases MDA level, increases the total antioxidant capacity and even reduces the OVX associated insulin resistance state [58]. This result is confirmed in the current study as there was improvement of the oxidative stress markers in group IV (E2 treated group) in comparison to group III (OVX model group). E2 exerts its antioxidant effects through different mechanisms. It increases and restores the intracellular glutathione level, has a role in the maintenance of normal cellular redox state and suppresses the production of superoxide anion [59, 60]. Moreover E2 has an activating effect on the intracellular soluble antioxidant defense system and it improves the electron transfer chain activity [60, 61].

There was improvement of the histological picture of the submandibular glands of animals representing group IV (E2 treated animals). Some acinar cells appeared with vesicular nuclei, while others had pyknotic nuclei and vacuolated cytoplasm. The granular contents

of the granular convoluted tubules were apparently less than that of the ovariectomized group with evident decrease in α SMA immunoreactivity. These results support the result of) [2]. They reported that E2 therapy could improve the OVX induced morphological changes in the submandibular gland. This can be explained by the possible antioxidant effect of E2 that can relieve or minimize the cellular changes induced by oxidative stress) [56]. Moreover, E2 has anti-apoptotic role through downregulation of gene expression of apoptotic genes [62] as well as its extra non-genomic effect through activation of signaling anti-apoptotic pathways [2].

The E2 treated animals showed a significant increase in SMP-30 mRNA gene expression in the current study, this result confirmed the anti-senescence role of estradiol which is in agreement with [63, 64]. It was reported that E2 induces gene expression at the level of transcription of the genes that antagonize, protect or delay cellular senescence [64], augment telomerase activity [65]. Additionally, E2 protects against the mitochondrial damage induced by H2O2 and hence delay the cellular senescence [66]. But the prolonged use of E2as a replacement therapy alone is not fully effective and non-preferable due to its previously known hazards [67].

CoQ10 is a lipo-soluble free radical scavenger [68]. It is well known for its antioxidant and anti-inflammatory effects and it is the most common type of Co Q in human tissue [69]. As it is a member of mitochondrial respiratory chain; it prevents and minimizes mitochondrial ROS production [70], increases the mass of mitochondria [71] and augments its function [67]. Its essential roles are energy conversion, antioxidant activity and antioxidant regenerator, cell growth stimulation, and cell death inhibition [69, 72]. The selection ofCoQ10 to be a complementary treatment of OVX induced salivary gland damage is based on the fact that CoQ10 level is lower in any condition of hypogonadism with lowered sex hormones levels including postmenopausal women [63, 64]. It is reported that Co Q10 decreases with the progress of age, its decline starts by the age of 30s in some tissues of human hence its role in prevention of aging process [73, 74]. The decrease in the availability in Co Q10 is correlated with the decrease in the fertility potentials in human [75].

The antioxidant activity of CoQ10 provides it a benefit of delaying cellular aging and senescence [76, 77]. Moreover, the main mechanism of anti-senescence of CoQ10 is through inhibition of the signaling pathways that is involved in senescence especially, AKt/mTOR pathway which is considered the main mediator of mesenchymal stem cell aging process [78, 79].

The results of the current study proved these helpful effects of CoQ10 in prevention and treatment of OVX induced submandibular gland damage. The ultrastructure picture, the biochemical and the molecular findings of group V (combined CoQ10 and E2 therapy group) demonstrated an effective therapy in the form of marked improvement of molecular findings as well as return of the immunohistochemical and histological picture nearly to normal.

Conclusion

Based upon the results of the present study, ovariectomy can induce histological changes in the submandibular gland with development of oxidative stress and induction of cellular senescence. Estrogen has a protective role but combined CoQ10 and E2 therapy could have a better effect in prevention and protection against OVX induced submandibular gland damage. Therefore, CoQ10 seems to be a promising antioxidant with significant therapeutic effects in the amelioration of the histological, immunohistochemical and molecular changes of the submandibular gland. Further studies are necessary to know the detailed mechanisms underlying the beneficial properties of CoQ10 and its clinical efficacy in prevention and treatment of postmenopausal tissue damage.

Disclosure of conflict of interest

None.

Address correspondence to: Ayman Z Elsamanoudy, Medical Biochemistry and Molecular Biology, Faculty of Medicine, Mansoura University, El-Gomhoria St., Mansoura, Egypt. Tel: +201065300733; +966595-062375; E-mail: ayman.elsamanoudy@gmail.com

References

[1] Carvalho VD, Silveira VÁ, do Prado RF, Carvalho YR. Effect of estrogen therapy, soy isoflavones, and the combination therapy on the submandibular gland of ovariectomized rats. Pathol Res Pract 2011; 207: 300-5.

[2] Da Y, Ni K, Wang K, Cui G, Wang W, Jin B, Bai W. A Comparison of the Effects of Estrogen and Cimicifuga racemosa on the Lacrimal Gland and Submandibular Gland in Ovariectomized Rats. PLoS One 2015; 10: e0121470.
[3] Streckfus GF, Baur U, Brown LJ, Baca C, Metter J, Nick T. Effects of estrogen status and aging on salivary flow rates in healthy Caucasian women. Gerontology 1998; 44: 32-39.
[4] Eliasson L, Carlén A, Laine M, Birkhed D. Minor gland and whole saliva in postmenopausal women using a low potency oestrogen (oestriol). Arch Oral Biol 2003; 48: 511-517.
[5] Agha-Hosseini F, Mirzaii-Dizgah I, Mansourian A, Khayamzadeh M. Relationship of stimulated saliva 17 beta-estradiol and oral dryness feeling in menopause. Maturitas 2009; 62: 197-9.
[6] Rowland BD, Denissov SG, Douma S, Stunnenberg HG, Bernards R and Peeper DS. E2F transcriptional repressor complexes are critical downstream targets of p19 (ARF)/p53-induced proliferative arrest. Cancer Cell 2002; 2: 55-65.
[7] Moiseeva O, Mallette FA, Mukhopadhyay UK, Moores A and Ferbeyre G. DNA damage signaling and p53-dependent senescence after prolonged beta-interferon stimulation. Mol Biol Cell 2006; 17: 1583-1592.
[8] Bhatia-Dey N, Kanherkar RR, Stair SE, Makarev EO, Csoka AB. Cellular Senescence as the Causal Nexus of Aging. Front Genet 2016; 7: 13.
[9] Fujita T, Inoue H, Kitamura T, Sato N, Shimosawa T and Maruyama N. Senescence marker protein-30 (SMP30) rescues cell death by enhancing plasma membrane Ca2+-pumping activity in Hep G2 cells. Biochem Biophys Res Commun 1998; 250: 374-380.
[10] Ishii K, Tsubaki T, Fujita K, Ishigami A, Maruyama N, Akita M. Immunohistochemical localization of senescence marker protein-30 (SMP30) in the submandibular gland and ultrastructural changes of the granular duct cells in SMP30 knockout mice. Histol Histopathol 2005; 20: 761-8.
[11] Handa S, Maruyama N, Ishigami A. Over-expression of Senescence Marker Protein-30 decreases reactive oxygen species in human hepatic carcinoma Hep G2 cells. Biol Pharm Bull 2009; 32: 1645-1648.
[12] Fukui M, Senmaru T, Hasegawa G, Yamazaki M, Asano M, Kagami Y, Ishigami A, Maruyama N, Iwasa K, Kitawaki J, Itoh Y, Okanoue T, Ohta M, Obayashi H, Nakamura N. 17β-Estradiol attenuates saturated fatty acid diet-induced liver injury in ovariectomized mice by up-regulating hepatic senescence marker protein-30. Biochem Biophys Res Commun 2011; 415: 252-257.
[13] Yamaguchi M. The anti-apoptotic effect of regucalcin is mediated through multisignaling pathways. Apoptosis 2013; 18: 1145-53.
[14] Santos-Ocana C, Do TQ, Padilla S, Navas P, Clarke CF. Uptake of exogenous coenzyme Q and transport to mitochondria is required for bc1 complex stability in yeast coq mutants. J Biol Chem 2002; 277: 10973-10981.
[15] Bentinger M, Brismar K, Dallner G. The antioxidant role of coenzyme Q. Mitochondrion 2007; 7 Suppl: S41-S50.
[16] Quinzii CM, Hirano M, DiMauro S. CoQ10 deficiency diseases in adults. Mitochondrion 2007; 7 Suppl: S122-S126.
[17] Ryo K, Ito A, Takatori R, Tai Y, Arikawa K, Seido T, Yamada T, Shinpo K, Tamaki Y, Fujii K, Yamamoto Y, Saito I. Effects of coenzyme Q10 on salivary secretion. Clin Biochem 2011; 44: 669-74.
[18] Kalyan S, Huebbe P, Esatbeyoglu T, Niklowitz P, Côté HC, Rimbach G, Kabelitz D. Nitrogen-bisphosphonate therapy is linked to compromised coenzyme Q10 and vitamin E status in postmenopausal women. J Clin Endocrinol Metab 2014; 99: 1307-13.
[19] Ulas M, Cay M. The effects of 17b-estradiol and vitamin E treatments on oxidative stress and antioxidant levels in brain cortex of diabetic ovariectomized rats. Acta Physiol Hung 2010; 97: 208-215.
[20] Saiki R, Lunceford AL, Shi Y, Marbois B, King R, Pachuski J, Kawamukai M, Gasser DL, Clarke CF. Coenzyme Q10 supplementation rescues renal disease in Pdss2kd/kd mice with mutations in prenyl diphosphate synthase subunit 2. Am J Physiol Renal Physiol 2008; 295: F1535-F1544.
[21] Waynforth HB. (1980): Experimental and surgical technique in the rat. Academic Press Inc.
[22] Angèle S, Jones C, Reis Filho JS, Fulford LG, Treilleux I, Lakhani SR, Hall J. Expression of ATM, p53, and the MRE11-Rad50-NBS1 complex in myoepithelial cells from benign and malignant proliferations of the breast. J Clin Pathol 2004; 57: 1179-1184.
[23] Redman RS. On approaches to the functional restoration of salivary glands damaged by radiation therapy for head and neck cancer, with a review of related aspects of salivary gland morphology and development. Biotech Histochem 2008; 83: 103-130.
[24] Bozzola JJ, Russell LD. Electron microscopy: principles and techniques for biologists. 2nd edition. Toronto, London: Jones and Bartlett Publishers; 1999.
[25] Yoshioka T, Kawada K, Shimada T, Mori M. Lipid peroxidation in maternal and cord blood and protective mechanism against activate-

doxygen toxicity in the blood. Am J Obst Gynecol 1979; 135: 372-376.
[26] Katalinic V, Modun D, Music I, Boban, M. Gender differences in antioxidant capacity of rat tissues determined by 2, 2 V-azinobis (3- ethylbenzothiazoline 6-sulfonate; ABTS) and ferric reducing antioxidant power (FRAP) assays. Comp Biochem Physiol C Toxicol Pharmacol 2005; 140: 47-52.
[27] Laurentino SS, Correia S, Cavaco JE, Oliveira PF, Rato L, Sousa M, Barros A, Socorro S. Regucalcin is broadly expressed in male reproductive tissues and is a new androgen-target gene in mammalian testis. Reproduction 2011; 142: 447-456.
[28] Arruda LF, Arruda SF, Campos NA, de Valencia FF, de Siqueira EM. Dietary Iron Concentration May Influence Aging Process by Altering Oxidative Stress in Tissues of Adult Rats. PLoS One 2013; 8: e61058.
[29] Machi JF, Dias Dda S, Freitas SC, de Moraes OA, da Silva MB, Cruz PL, Mostarda C, Salemi VM, Morris M, De Angelis K, Irigoyen MC. Impact of aging on cardiac function in a female rat model of menopause: role of autonomic control, inflammation, and oxidative stress. Clin Interv Aging 2016; 11: 341-50.
[30] Hershko C. Mechanism of iron toxicity and its possible role in red cell membrane damage. Semin Hematol 1989; 26: 277-285.
[31] Mano J. Reactive carbonyl species: their production from lipid peroxides, action in environmental stress, and the detoxification mechanism. Plant Physiol Biochem 2012; 59: 90-7.
[32] Ho E, Karimi Galougahi K, Liu CC, Bhindi R, Figtree GA. Biological markers of oxidative stress: applications to cardiovascular research and practice. Redox Biology 2013; 1: 483-491.
[33] Shimomura K, Shimizu H, Tsuchiya T, Abe Y, Uehara Y, Mori M. Is leptin a key factor which develops obesity by ovariectomy? Endocr J 2002; 49: 417-423.
[34] Gulcelik NE, Halil M, Ariogul S, Usman A. Adipocytokines and aging: adiponectin and leptin. Minerva Endocrinol 2013; 38: 203-210.
[35] Wronska A, Lawniczak A, Wierzbicki PM, Goyke E, Sledzinski T, Kmiec Z. White adipose tissue depot-specific activity of lipogenic enzymes in response to fasting and refeeding in young and old rats. Gerontology 2015; 61: 448-455.
[36] Andersson U, Tracey KJ. Neural reflexes in inflammation and immunity. J Exp Med 2012; 209: 1057-1068.
[37] Benedusi V, Martini E, Kallikourdis M, Villa A, Meda C, Maggi A. Ovariectomy shortens the life span of female mice. Oncotarget 2015; 6: 10801-10811.
[38] Small DM, Bennett NC, Roy S, Gabrielli BG, Johnson DW, Gobe GC. Oxidative stress and cell senescence combine to cause maximal renal tubular epithelial cell dysfunction and loss in an in-vitro model of kidney disease. Nephron Exp Nephrol 2012; 122: 123-130.
[39] Tang Y, Li S, Zhang P, Zhu J, Meng G, Xie L, Yu Y, Ji Y, Han Y. Soy Isoflavone Protects Myocardial Ischemia/Reperfusion Injury through Increasing Endothelial Nitric Oxide Synthase and Decreasing Oxidative Stress in Ovariectomized Rats. Oxid Med Cell Longev 2016; 5057405.
[40] Duchen MR. Mitochondria and calcium: from cell signalling to cell death. J Physiol 2000; 529: 57-68.
[41] Ermak G, Davies KJA. Calcium and oxidative stress: from cell signaling to cell death. Mol Immunol 2001; 38: 713-721.
[42] Ishigami A, Kondo Y, Nanba R, Ohsawa T, Handa S, Kubo S, Akita M, Maruyama N. SMP30 deficiency in mice causes an accumulation of neutral lipids and phospholipids in the liver and shortens the life span. Biochem Biophys Res Commun 2004; 315: 575-580.
[43] Segawa A, Loffredo F, Puxeddu R, Yamashina S, Testa Riva F, Riva A. Cell biology of human salivary secretion. Eur J Morphol 2000; 38: 237-241.
[44] Jeong J, Baek H, Kim YJ, Choi Y, Lee H, Lee E, Kim ES, Hah JH, Kwon TK, Choi IJ, Kwon H. Human salivary gland stem cells ameliorate hyposalivation of radiation-damaged rat salivary glands. Exp Mol Med 2013; 45: e58.
[45] Uyanıkgil Y, Türkkozan NY, Balcıoğlu HA, Ateş U, Özel S. The effects of ovariectomy on the submandibular gland in young female adult rats. Ege Tıp Dergisi/Ege Journal of Medicine 2011; 50: 7-11.
[46] Kusunoki T, Shiraishi H, Murata K, Nishida N, Tomura T. Apoptosis and estrogen on aging changes of female rat parotids. Aging cell Acta Med Kinki Univ 2004; 29: 27-30.
[47] Younis R, AbouElkhier M, Mourad M, Elnahas W. Ultrastructural changes in the parotid gland of rats after intraglandular injection of botulinum toxin A. Annals of Oral & Maxillofacial Surgery 2013; 1: 38.
[48] Stramandinoli-Zanicotti RT, Sassi LM, Schussel JL, Torres MF, Funchal M, Smaniotto GH, Dissenha JL, Carvalho AL. Effect of fractionated radiotherapy on the parotid gland: an experimental study in Brazilian minipigs. Int Arch Otorhinolaryngol 2013; 17: 163-7.
[49] Mohamed DA, Elnegris HM, Wahdan RA. Histological effect of ovariectomy and estrogen replacement on parotid gland of adult albino rat. J Histol Histopathol 2015; 2: 23.
[50] Petschnik AE, Fell B, Kruse C, Danner S. The role of alpha-smooth muscle actin in myogenic differentiation of human glandular stem cells and their potential for smooth muscle cell re-

placement therapies. Expert Opin Biol Ther 2010; 10: 853-861.
[51] Hasegawa A, Nakahara H, Kinoshita M, Asahara H, Koziol J, Lotz MK. Cellular and extracellular matrix changes in anterior cruciate ligaments during human knee aging and osteoarthritis. Arthritis Res Ther 2013; 15: R29.
[52] da Costa NM, Correa RS, Júnior IS, Figueiredo AJ, Vilhena KF, Farias-Junior PM, Teixeira FB, Ferreira NM, Pereira-Júnior JB, Dantas Kd, da Silva MC, Silva-Junior AF, Alves-Junior Sde M, Pinheiro Jde J, Lima RR. Physical, Chemical, and Immunohistochemical Investigation of the Damage to Salivary Glands in a Model of Intoxication with Aluminium Citrate. Int J Environ Res Public Health 2014; 11: 12429-40.
[53] Kis K, Liu X, Hagood JS. Myofibroblast differentiation and survival in fibrotic disease. Expert Rev Mol Med 2011; 13: e27.
[54] Luo J, Hosoki K, Bacsi A, Radak Z, Hegde ML, Sur S, Boldogh I. 8-Oxoguanine DNA glycosylase-1-mediated DNA repair is associated with Rho GTPase activation and α-smooth muscle actin polymerization. Free Radic Biol Med 2014; 73: 430-438.
[55] Sueblinvong V, Neujahr DC, Mills ST, Roser-Page S, Ritzenthaler JD, Guidot D, Rojas M, Roman J. Predisposition for disrepair in the aged lung. Am J Med Sci 2012; 344: 41-51.
[56] Sueblinvong V, Neveu WA, Neujahr DC, Mills ST, Rojas M, Roman J, Guidot DM. Aging promotes pro-fibrotic matrix production and increases fibrocyte recruitment during acute lung injury. Adv Biosci Biotechnol 2014; 5: 19-30.
[57] Bednarek-Tupikowska G, Bohdanowicz-Pawlak A, Bidzinska B, Milewicz A, Antonowicz-Juchniewicz J, Andrzejak R. Serum lipid peroxide levels and erythrocyte glutathione peroxidase and superoxide dismutase activity in premenopausal and postmenopausal women. Gynecol Endocrinol 2001; 15: 298-303.
[58] Serviddio G, Loverro G, Vicino M, Prigigallo F, Grattagliano I, Altomare E, Vendemiale G. Modulation of endometrial redox balance during the menstrual cycle: relation with sex hormones. J Clin Endocrinol Metab 2002; 87: 2843-2848.
[59] Abbas AM, Elsamanoudy AZ. Effects of 17β-estradiol and antioxidant administration on oxidative stress and insulin resistance in ovariectomized rats. Can J Physiol Pharmacol 2011; 89: 497-504.
[60] Békési G, Kakucs R, Várbíró S, Rácz K, Sprintz D, Fehér J, Székács B. In vitro effects of different steroid hormones on superoxide anion production of human neutrophil granulocytes. Steroids 2000; 65: 889-94.
[61] Mancini A, Raimondo S, Persano M, Di Segni C, Cammarano IM, Gadotti G, Silvestrini A, Pontecorvi A, Meucci E. Estrogens as Antioxidant Modulators in Human Fertility. Int J Endocrinol 2013; 2013: 607939.
[62] Nilsen J. Estradiol and neurodegenerative oxidative stress. Front Neuroendocrinol 2008; 29: 63-475.
[63] Fu Z, Zou F, Deng H, Zhou H, Liu L. Estrogen protects SGC7901 cells from endoplasmic reticulum stress-induced apoptosis by the Akt pathway. Oncol Lett 2014; 7: 560-4.
[64] Mancini A, Leone E, Festa R, Grande G, Silvestrini A, de Marinis L, Pontecorvi A, Maira G, Gianpaolo L, Meucci E. Effects of testosterone on antioxidant systems in male secondary hypogonadism. J Androl 2008; 29: 622-629.
[65] Mancini A, Festa R, Raimondo S, Pontecorvi A, Littarru GP. Hormonal Influence on Coenzyme Q10 Levels in Blood Plasma. Int J Mol Sci 2011; 12: 9216-9225.
[66] Imanishi T, Tsujioka H, Akasaka T. Endothelial progenitor cell senescence--is there a role for estrogen? Ther Adv Cardiovasc Dis 2010; 4: 55-69.
[67] Ruan Y, Wu S, Zhang L, Chen G, Lai W. Retarding the senescence of human vascular endothelial cells induced by hydrogen peroxide: effects of 17beta-estradiol (E2) mediated mitochondria protection. Biogerontology 2014; 15: 367-75.
[68] Sandhir R, Sethi N, Aggarwal A, Khera A. Coenzyme Q10 treatment ameliorates cognitive deficits by modulating mitochondrial functions in surgically induced menopause. Neurochem Int 2014; 74: 16-23.
[69] Kang D, Hamasaki N. Mitochondrial oxidative stress and mitochondrial DNA. Clin Chem Lab Med 2003; 41; 1281-1288.
[70] Esrefoglu M. Experimental and clinical evidence of antioxidant therapy in acute pancreatitis. World J Gastroenterol 2012; 18: 5533-5541.
[71] Chen CC, Liou SW, Chen WC, Hu FR, Wang IJ, Lin SJ. Coenzyme Q10 reduces ethanol-induced apoptosis in corneal fibroblasts. PLoS One 2011; 6: e19111.
[72] Noh YH, Kim KY, Shim MS, Choi SH, Choi S, Ellisman MH, Weinreb RN, Perkins GA, Ju WK. Inhibition of oxidative stress by coenzyme Q10 increases mitochondrial mass and improves bioenergetic function in optic nerve head astrocytes. Cell Death Dis 2013; 4: e820.
[73] Crane FL. Biochemical functions of coenzyme Q10. J Am Coll Nutr 2001; 20: 591-598.
[74] Morre DM, Guo F, Morre DJ. An aging-related cell surface NADH oxidase (arNOX) generates superoxide and is inhibited by coenzyme Q. Mol Cell Biochem 2003; 254: 101-109.

[75] Miles MV, Horn PS, Tang PH, Morrison JA, Miles L, DeGrauw T, Pesce AJ. Age-related changes in plasma coenzyme Q10 concentrations and redox state in apparently healthy children and adults. Clin Chim Acta 2004; 347: 139-144.

[76] Ben-Meir A, Burstein E, Borrego-Alvarez A, Chong J, Wong E, Yavorska T, Naranian T, Chi M, Wang Y, Bentov Y, Alexis J, Meriano J, Sung H, Gasser DL, Moley KH, Hekimi S, Casper RF, Jurisicova A. Coenzyme Q10 restores oocyte mitochondrial function and fertility during reproductive aging. Aging Cell 2015; 14: 887-895.

[77] Tarry-Adkins JL, Blackmore HL, Martin-Gronert MS, Fernandez-Twinn DS, McConnell JM, Hargreaves IP, Giussani DA, Ozanne SE. Coenzyme Q10 prevents accelerated cardiac aging in a rat model of poor maternal nutrition and accelerated postnatal growth. Mol Metab 2013; 2: 480-90.

[78] Ma D, Stokes K, Mahngar K, Domazet-Damjanov D, Sikorska M, Pandey S. Inhibition of stress induced premature senescence in presenilin-1 mutated cells with water soluble Coenzyme Q10. Mitochondrion 2014; 17: 106-115.

[79] Zhang D, Yan B, Yu S, Zhang C, Wang B, Wang Y, Wang J, Yuan Z, Zhang L, Pan J. Coenzyme Q10 Inhibits the Aging of Mesenchymal Stem Cells Induced by D-Galactose through Akt/mTOR Signaling. Oxid Med Cell Longev 2015; 2015: 867293.